3. Cosmology and the Origin and Evolution of Galaxies

3.1 Introduction

In 1997 the U.S. National Research Council's Committee on Astronomy and Astrophysics (CAA) prioritized the most important scientific questions in space astronomy and astrophysics to be addressed during the subsequent decade. The highest four priorities were:

1. the determination of the geometry and content of the universe by measurement of the fine-scale anisotropies of the cosmic microwave background;
2. the investigation of galaxies near the time of their formation at very high-redshift;
3. the detection and study of planets around nearby stars;
4. the measurement of the properties of black holes of all sizes.

The capabilities of the LMT and that part of the LMT science-program devoted to studies of the formation and evolution of structure at high-redshift, described in this chapter, are thus entirely consistent with this important strategic report from the CAA. Moreover, these important scientific questions are uniquely relevant, for the reasons described below, to astronomy in general.

Observational evidence suggests that much of the ongoing star formation in the universe takes place in the dusty, heavily obscured interstellar medium (ISM) in galaxies. This star formation activity can therefore be hidden from ultraviolet, optical, and infrared surveys. A more transparent view of the universe, however, can be provided by sub-millimeter and millimeter-wavelength observations, which are insensitive to the obscuring effects of dust. Millimeter astronomy thus offers a unique opportunity to challenge the accepted scenarios that describe our current understanding of the physical processes that drive the formation of structure in the universe, and control its subsequent evolution into the galaxies and clusters that we see today.

Significant theoretical, experimental, and observational effort has been focused on addressing these fundamental cosmological questions. When the universe was less than 10% of its current age, the first galaxies had already formed from the first generations of stars, which then proceeded to enrich the primeval ISM with heavy elements and the other by-products of star formation. The physical environment of the high-redshift universe (and therefore presumably in high-redshift galaxies) is potentially very different
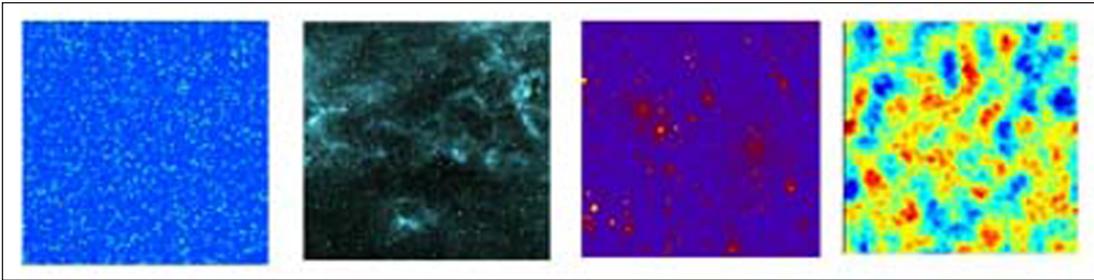
Figure 3.1 From left to right: Mm-wavelength simulations of a strongly evolving and clustered starburst galaxy population, Galactic cirrus, Sunyaev-Zel'dovich clusters, and fluctuations in the Cosmic Microwave Background. These simulations are merged to provide realistic maps of the extragalactic sky, which can be combined with an instrument and telescope simulator to estimate the feasibility of possible LMT surveys[1].

from that observed today, and thus it may be naive to assume that the detailed process of star formation and its efficiency are identical over all cosmic epochs. Thus, in order to understand the formation and evolution of galaxies, we must also understand the formation and evolutionary history of stars (Chapter 5), and then place the galaxies and clusters in the context of the larger-scale distributions of matter that have evolved from the initial structures observed in the cosmic microwave background anisotropies.

3.2 The History of Optically Obscured High-Redshift Star Formation

Violent star formation in dusty, optically obscured galaxies manifests itself in far-infrared (FIR) to mm-wavelength observations. Because the strong FIR emission peak is increasingly shifted into the sub-mm and millimeter range as the distance and hence redshift (z) increases, millimeter wavelength observations are able to trace the evolution of star formation in dusty galaxies throughout a large volume of the high-redshift universe (in principle with as much ease at redshift $z \sim 8$ as at $z \sim 1$), and therefore back to extremely early epochs (Figure 3.2). Given a large accessible volume from mm surveys, it is possible to test the important question of whether galaxies observed at these wavelengths represent the rapid formation of massive (elliptical) systems in a single violent collapse of the highest-density peaks of the underlying large-scale matter distribution, or whether they are built over a longer period from the continuous merging of lower-mass systems with much more modest rates of star formation.
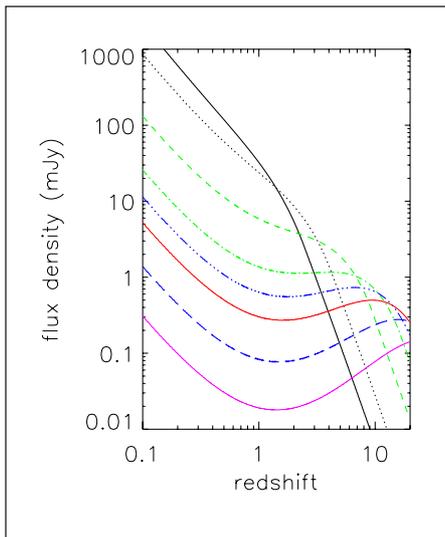

Figure 3.2 (a) The effect of redshift on flux density at far infrared to mm wavelengths for an object similar to the ultraluminous galaxy Arp220. From top to bottom (at a redshift of z=0.1) the colored curves show this effect at 160, 250, 500, 850, 1100, 1400, 2100, 3300 microns, respectively[2].

A major scientific goal for the LMT is therefore to exploit its higher angular resolution, sensitivity and mapping speed, compared to all of the existing facilities and most
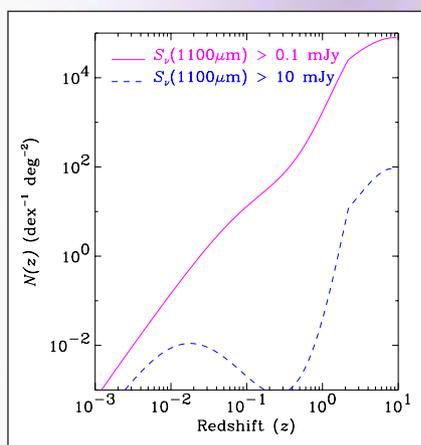
Figure 3.2 (b) The predicted redshift distribution of dusty starburst galaxies for representative LMT surveys. The deep, small-area surveys (solid line) will be dominated by a high-redshift (z > 2) population of sources, while the shallower and wider-area LMT surveys (dashed line) will contain a bimodal population that also includes bright galaxies in the local universe (z < 0.05)[2].

of the new experiments (e.g., Table 2.3), in the effort to understand the evolutionary history of the galaxy populations that dominate the integrated FIR-mm extragalactic background emission.

More specifically, the LMT will conduct a range of narrow, confusion-limited surveys and larger-area, shallower surveys of the high-redshift universe at mm wavelengths. Together with complementary multi-wavelength observations, these data will (i) identify the individual galaxies that supply that part of the FIR-mm background (~ 50% of the integrated energy budget of the universe emitted by discrete sources) and determine their redshifts; (ii) measure their individual bolometric luminosities, star formation rates and the evolution of their integrated luminosity functions; (iii) determine the fraction of active galactic nuclei (AGN) in the various FIR-mm galaxy populations; (iv) measure the spatial clustering properties of these galaxies; and (v) characterize the multi-wavelength spectroscopic and continuum properties of these dusty galaxy populations.

3.2.1 Cosmological Surveys with the LMT

The first generations of cosmological surveys at mm wavelengths[3,4] have been conducted primarily with the SCUBA and MAMBO cameras, which both use modest-sized bolometer arrays (~100 pixels), on the 15 m JCMT and 30 m IRAM telescopes, respectively. These various mm surveys, which covered areas ranging from a few square arcminutes to 0.5 square degree, have contributed significantly to the first efforts to understand the history of obscured star formation in the early universe. Use of these observations alone,
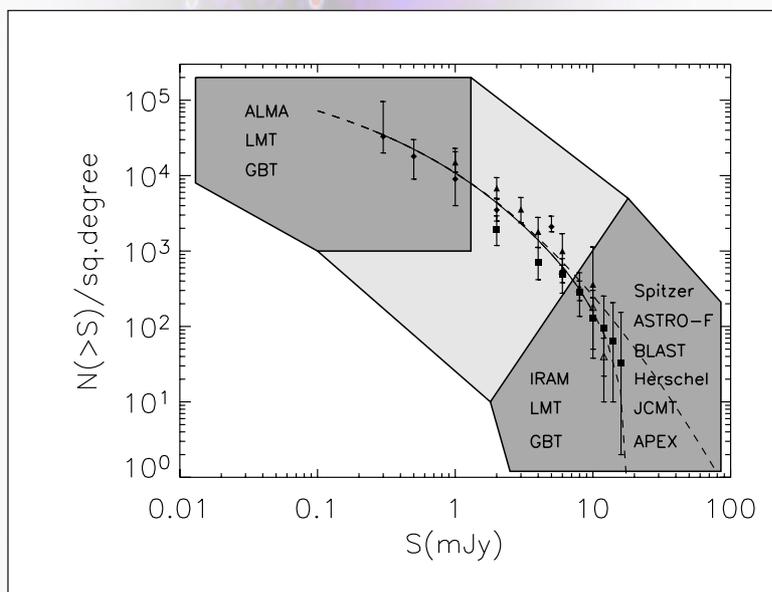

Figure 3.3 Extragalactic 850 μm source-counts as a function of flux measure from the SCUBA surveys. The solid-line represents one of many possible strongly-evolving models that fit the 850 μm data. The measured source-counts cover a narrow range of flux densities (~ 0.5 – 12 mJy) and therefore leave two unexplored regions (shown as dark-grey shaded polygons) populated by the numerous, faint galaxies below the existing observational confusion limits, and the brightest, but rarer galaxies that can only be detected in the widest-area surveys[5].

however, cannot accurately determine the evolution and large-scale distribution of the mm galaxy population. Figure 3.3 illustrates the two fundamental reasons why this is the case: first, the measured sub-mm source-counts from the combined extragalactic surveys cover only a narrow range of source brightness; second, the uncertainty in source count is substantial, because the total number of sources detected with a signal-to-noise of at least four is less than 100. Thus, with these limited statistics it is difficult to determine the flux-density at which the faint-end source-counts converge, and therefore determine the contribution of this mm population to the extragalactic background emission (Section 3.2.2). Galaxy clustering and the small areas covered by the surveys also make the count of faint sources uncertain, and the rareness of the brightest sources makes it difficult to ascertain whether there is a cut-off in the evolving luminosity function and redshift distribution of the mm population.
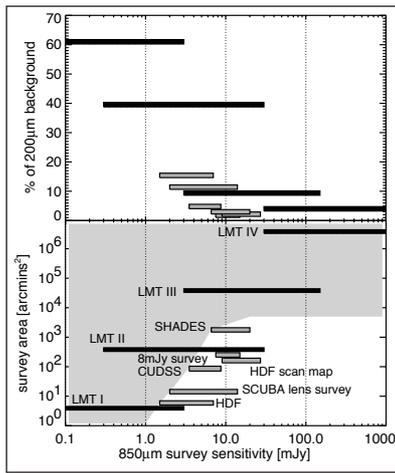

Figure 3.4 Cosmological surveys with the LMT: small area and very deep, very broad but shallower, and intermediate surveys are planned. The corresponding fraction of the resolved far infrared background emission is illustrated in the upper panel[6].

The practical reasons for the above limitations of the existing experiments can be summarized as follows: restricted wavelength coverage (enforced by the few FIR-mm atmospheric windows available to ground-based observatories); low spatial resolution (resulting in both a high extragalactic confusion limit and poor positional accuracy); restricted field-of-view with the current mm bolometer arrays (typically 5 square arcmin); and low system sensitivity (a combination of instrument noise, size of telescope aperture and telescope surface accuracy, sky transmission, and sky noise) that restrict even the widest and shallowest mm surveys to areas smaller than half a square degree. Hence, the existing mm observations are necessarily only sensitive to the most luminous and massive star-forming galaxies ($L_{FIR} \sim 3 \times 10^{12} L_{sun}$, corresponding to a star formation rate (SFR) greater than 300 solar masses per year), provided that the population is dominated by galaxies at redshifts greater than 1 (an assumption that is consistent with the spectroscopic and photometric redshifts).

Cosmological surveys with the LMT will improve upon all of the above limitations (Figure 3.4). The LMT will use its very high mapping speed, sensitivity, and angular resolution to measure the surface density and clustering properties of dusty starburst galaxies detected between 850 μm and 3 mm over a wide dynamic-range of flux densities, making it one of the most powerful of all the future FIR-mm experiments[5]. The capabilities of
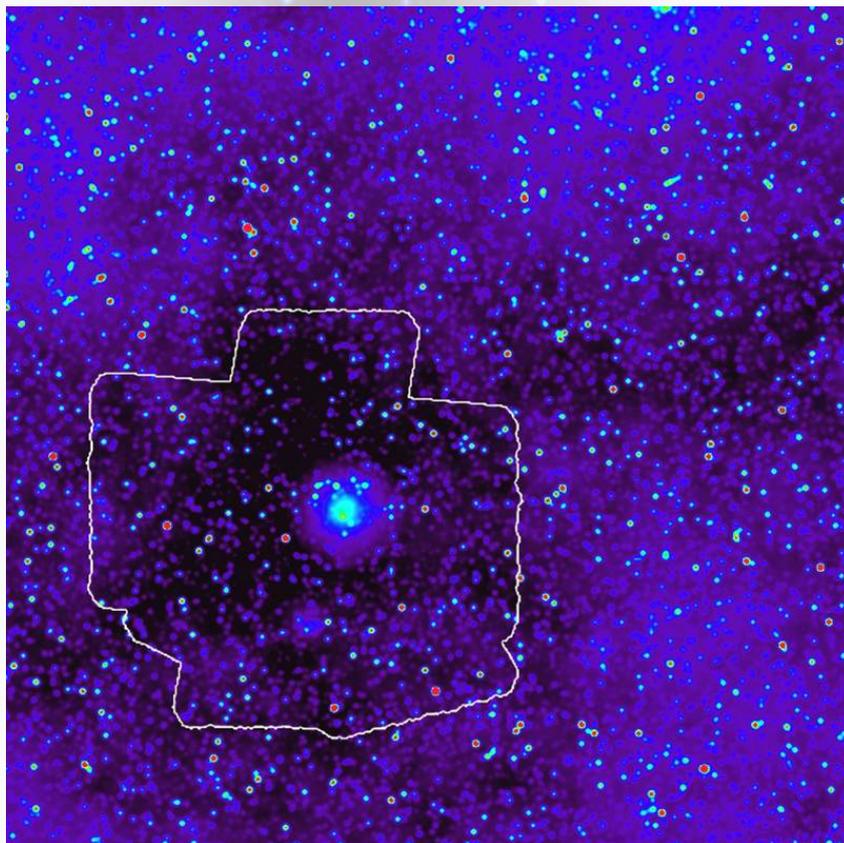
the LMT allow it to simultaneously search for and detect the optically-obscured galaxies with far more modest FIR luminosities ($L_{FIR} \sim 10^{11} L_{sun}$) and star formation rates (~10-50 solar masses per year) compared to previous surveys, as well as discover the brightest and rarest mm sources in the high-redshift universe. For example, a search for the most extreme star-forming galaxies (SFR >> 5000 solar masses per year), associated perhaps with the rapid formation of a massive elliptical in less than a few billion years, would require a sub-mm survey covering > 100 square degrees before a statistically significant result could be achieved.

3.2.2 Resolving the Far-Infrared-to-Millimeter-Wavelength Extragalactic Background

The integrated FIR-mm emission from all the galaxies in the universe peaks at ~ 250 μm and contributes approximately 50% of the total radio-X-ray extragalactic background light, and hence it is clearly a component that needs to be spatially resolved and understood. It is also important to note that << 1 square degree of the extragalactic sky has been mapped at mm wavelengths with sufficient resolution and sensitivity to begin the task of resolving a major fraction of this background emission. For example, despite eight years of intense effort to map the mm sky with ground-based telescopes, it is only in the deepest SCUBA surveys (rms > 0.5 mJy at 850 μm) that a significant fraction (≥ 30%) of the 850 μm background has been resolved into discrete galaxies[3,4], yet these same deep surveys have only observed ≤ 100 square arcmin in total. Furthermore, an extrapolation of the SCUBA and

Figure 3.5 Simulated emission from extra-galactic point sources at 1.1 mm for an area 0.5 x 0.5 square degrees, including contributions from the spectral Sunyaev-Zel'dovich increment caused by the thermal effect in the cluster near the map center (the extended source) and foreground Galactic dust ("cirrus"). More than 100 starburst galaxies would be detected in a 2-hour integration with AzTEC in the outlined region[1].

MAMBO source-counts to shorter submm wavelengths indicates that the same populations of galaxies detected in these deepest surveys at 850 μm and 1.1 mm contribute less than 15% of the FIR (250 μm) background emission, while the combined shallower (rms ~ 2.5 mJy at 850 μm) and wider-area (~ 2000 square arcmin) mm surveys provide only a few percent of the FIR background[6].

The LMT, which will be the largest single-aperture telescope operating at ~ 1 mm, will have an extremely low confusion-limit due to extragalactic sources. The opportunity to resolve the entire millimeter wavelength background into individual galaxies is thus well within the capabilities of the LMT and the first-light continuum camera, AzTEC. In Figure 3.4 we indicate the range of sensitivities and areas of sky that can be mapped in individual LMT surveys, and also the fraction of the FIR-mm background that can be resolved in each survey.
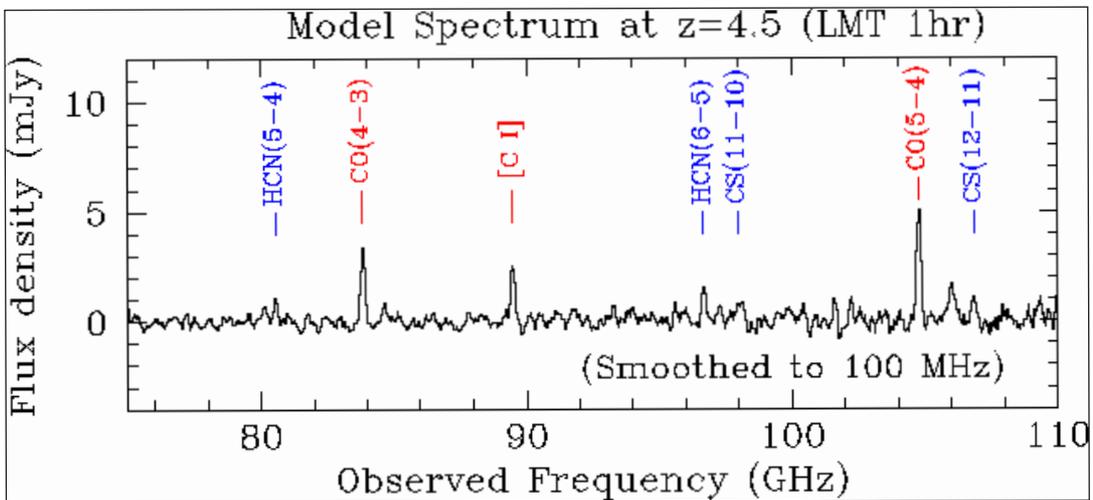

Figure 3.6 Simulated spectrum of a z = 4.5 mm galaxy after one hour of observation using the Redshift Search Receiver on LMT, assuming a system temperature of 100 K. The flux density of CO lines is based on measured line strengths of the z = 4.4 quasi-stellar object BRI 1335-0417. The brightness of other lines is based on average relative ratios observed in nearby luminous infrared galaxies[11].

3.2.3 Measuring the Redshift Distribution of Optically Obscured Galaxies with the LMT

Understanding the angular clustering properties and surface-density of mm-wavelength sources, and their contribution to the extragalactic background, is only part of the necessary information to understand the evolutionary properties of this population. It is also essential to accurately measure or constrain their redshift distribution. The extremely dusty ISM associated with star formation in this population of mm-wavelength galaxies makes it difficult to unambiguously identify their counterparts in optical and IR surveys. In recent years there has been considerable effort in assess-

ing whether broad continuum features in the spectral energy distributions (SEDs) of mm galaxies at rest-frame mid-IR to radio wavelengths can provide photometric-redshifts with sufficient accuracy[7]. There has also been some success in the measurement of optical and IR spectroscopic redshifts for a fraction of the bright mm galaxies ($S_{850\mu m} > 5$ mJy) with reliable radio counterparts[8]. Radio interferometric data help refine the positions of the mm galaxies, which allows the optical and IR counterparts to be identified with greater security and the spectroscopic observations to be undertaken with more confidence. The redshift-distribution determined from the radio-FIR photometric-colors and spectroscopic observations indicates that more than 60% of the brightest mm galaxies lie between redshifts z =1.8 - 3.5[8,9]. If we take into account the small fraction (< 10%) of the sub-mm background that corresponds to these bright sub-mm sources, however, it is immediately apparent that some other method has to be found in order to measure the redshifts for the fainter mm population that dominates the contribution to the extragalactic background emission.

The unique capabilities of the LMT and its suite of instrumentation provide an exciting solution to the problem of measuring the redshifts of the mm population of optically obscured galaxies. It has been demonstrated that dusty mm galaxies at high-redshift also contain enormous reservoirs of molecular gas (mass of $H_2 \sim 10^{10}$ - 10^{11} solar masses) that fuel the high rates of star formation[10]. Given these expected gas masses, the LMT has sufficient sensitivity to conduct a blind-search for molecular-line emission from the rotational transitions of carbon monoxide (CO) in the galaxies identified in the LMT blank-field surveys.

In order to conduct this molecular-line search, the LMT is building an ultra-wide-bandwidth receiver for operation in the 90 GHz window (Section 8.3.2). With an instantaneous bandwidth $\Delta v \sim 36$ GHz, this spectral-line receiver is ideally suited to a search for redshifted CO-lines. Since the frequency separation of the line transitions of CO-emission in the rest-frame is 115.27 GHz, then the observed frequency-separation, 115.27 GHz/(1+z), will provide an unambiguous redshift for the mm galaxies without the prior need for any optical, IR or radio galaxy counterpart. Assuming that the LMT provides sufficient sensitivity to detect molecular-line transitions from this population of dusty starburst galaxies, we can expect to detect at least one CO line regardless of the redshift of the galaxy. The only exception is if an individual galaxy lies in the redshift range between 0.4 and 1.0, where none of the CO lines are found within the frequency range of the Redshift Search Receiver. On the other hand, such galaxies
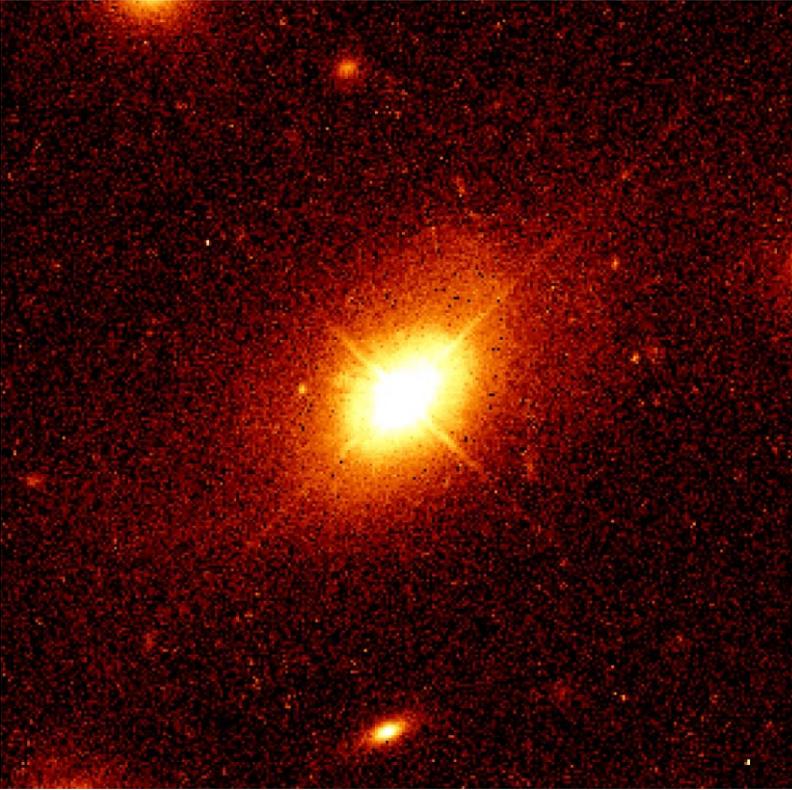
Figure 3.7 An HST image of a quasar[15].

should be easily recognized by their brightness at other wavelengths, and emission lines of other molecular species should be bright enough to yield a correct redshift. The detection of a single CO line is not sufficient to measure a spectroscopic redshift, but it will allow a constrained search for a second CO line for confirmation. Alternatively, for redshifts $z > 3.2$ we can expect either two CO lines, or a CO line and CI line in the 90 GHz window and hence a determination of a secure spectroscopic redshift for a mm galaxy from a single LMT observation, without the prior need for the identification of the optical, IR or radio counterpart.

The CO-line spectroscopic data measured by the LMT for individual mm-detected galaxies will therefore efficiently determine the redshift distribution of the population. Taken together with the two-dimensional LMT surveys describing their angular distribution, it will be possible to measure the spatial clustering of these luminous starburst galaxies over a wide range of redshifts and cosmological epochs. Furthermore, once an accurate spectroscopic redshift is measured for a mm galaxy, the LMT can utilize its narrower bandwidth receivers to make higher spectral-resolution observations to resolve the line-profile, and hence estimate the rotational velocity of the gas and infer a dynamical gas-mass.

These collective results from the continuum extragalactic surveys and the spectroscopic follow-up at mm wavelengths will place very strong constraints on the evolutionary history of star formation in this important galaxy population, and challenge the currently accepted scenarios for massive-galaxy formation.

3.3 High-Redshift Active Galactic Nuclei

The host galaxies of powerful active galactic nuclei (AGN) at all redshifts contain luminous radio sources and/or optical quasi-stellar objects (QSOs). In many cases large masses of molecular gas and dust have been detected[12]. AGN therefore provide important examples of galaxies that simultaneously exhibit both nuclear accretion activity onto black holes, and high rates of nuclear and/or circum-nuclear star formation.

Optical and IR imaging of powerful AGN at low-redshift ($z < 0.3$) demonstrate that they are hosted exclusively in massive elliptical galaxies[13]. Although at higher redshifts ($z \sim 2\text{-}3$) there is currently no morphological confirmation, the optical and IR luminosities of the high-z hosts of AGN are also consistent with those of first-ranked ellipticals[14].
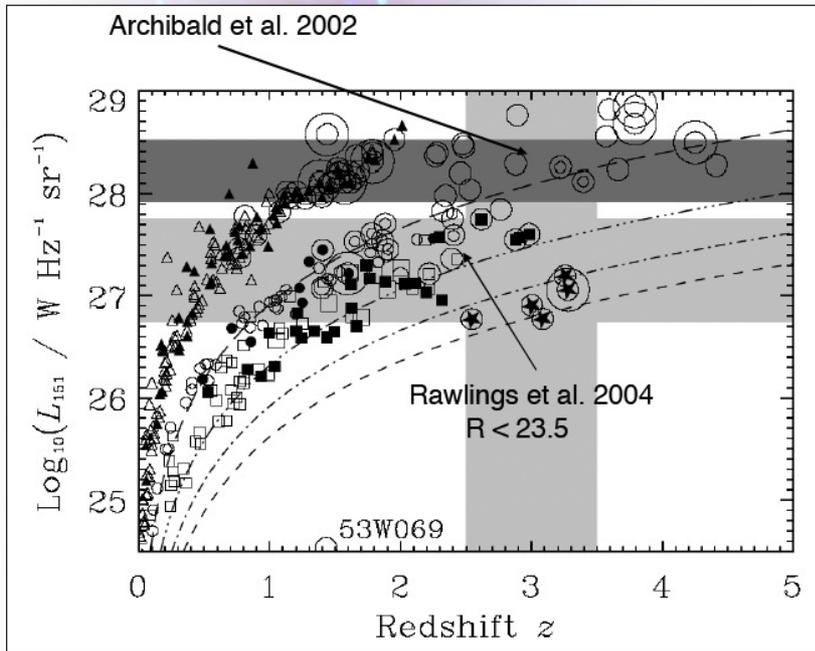

Figure 3.8 Radio luminosity at 151 MHz as a function of redshift for various surveys of radio galaxies and quasars. Shaded regions illustrate the possibility of selecting certain ranges of objects for study with the LMT[2, 17, 35].

Both active and inactive galaxies indicate a tight relationship between the mass of the spheroid (elliptical) and the mass of the central black hole[16]. This supports the idea that all galaxies, including our own Milky Way, have experienced a phase of AGN activity in their evolutionary histories, possibly associated with a major epoch of star formation. Thus, the study of the hosts of powerful AGN offers the opportunity to study the connection between the formation and evolution of black holes and the formation and evolution of elliptical galaxies (or, more generally, the spheroids in galaxies).

Using the LMT at mm wavelengths, we can study the non-thermal synchrotron emission from the AGN in radio-loud quasars, flat-spectrum radio galaxies, and the beamed blazar population; and the thermal continuum emission from dust heated by star formation and the molecular-gas content in the host galaxies of the radio-quiet quasars or steep-spectrum radio galaxies. Since ~ 90% of the entire AGN population are radio-quiet

sources, the LMT studies will reflect this dominance and concentrate their observational effort on the detection of gas and dust in the hosts of radio-quiet AGN. Due to the high point-source sensitivity and fast mapping-speed of the LMT, the mm-wavelength surveys of AGN are expected to be divided into two significant programs: (1) point-source photometry and molecular-line observations of a large unbiased sample of > 3000 AGN at all redshifts; and (2) imaging of the environments of AGN at $1 < z < 6$.
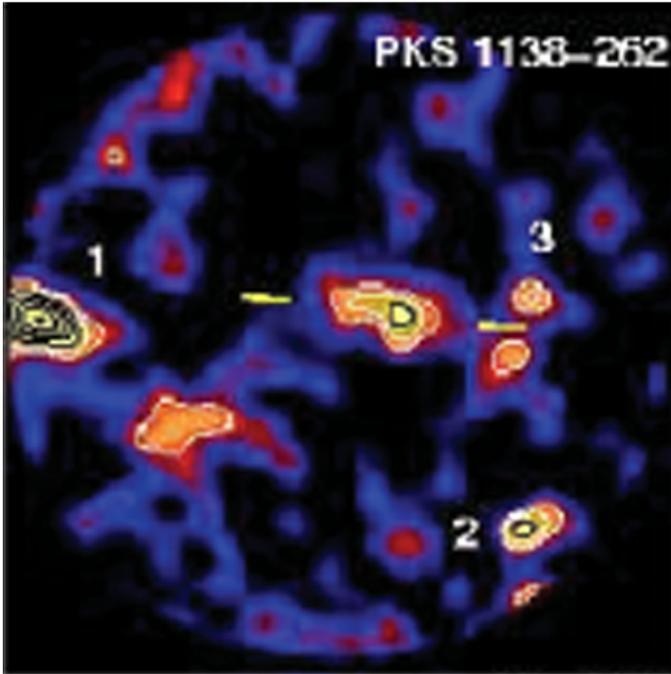
Figure 3.9 (a) Structure around the radio galaxy PKS1138-262 found with SCUBA at the JCMT[20]. The galaxies detected seem to be aligned with the radio jet, marked in the figure with the two yellow lines.
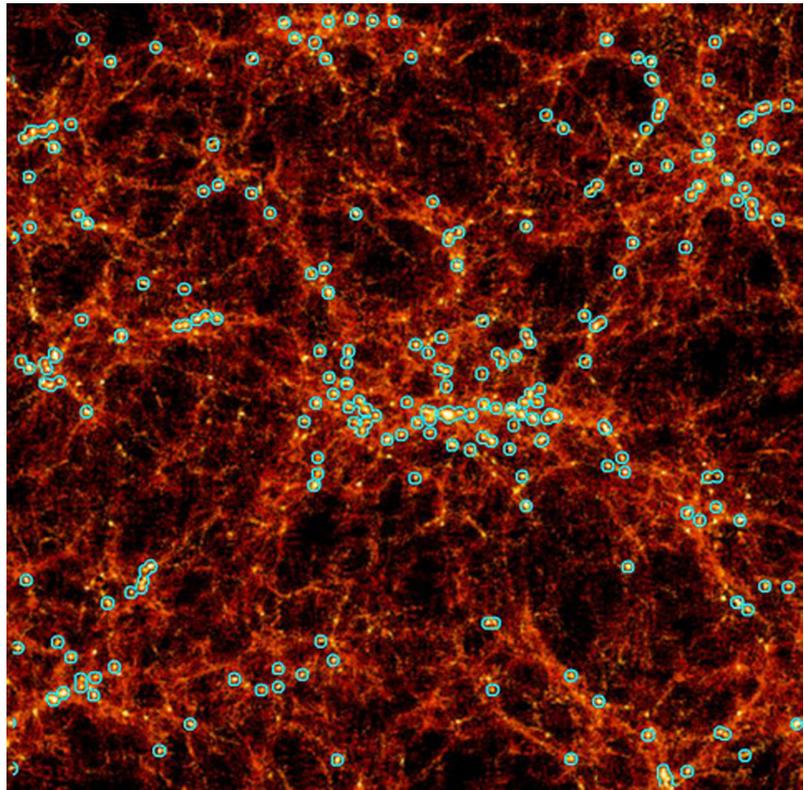

Figure 3.9 (b) 30′ x 30′ simulation at $z = 3$ of the progenitor of a rich cluster of galaxies[21]. The circles mark the position of the halos of massive galaxies whose size is about 60% of the SCUBA field. The LMT with AzTEC will be able to map the whole area of such a cluster progenitor and trace the large scale filaments.

3.3.1 Continuum-Emission and Molecular-Line Surveys of AGN

Previous mm-wavelength observations of AGN at $2 < z < 5$ have demonstrated that they are hosted in massive and young galaxies, and that the hosts are chemically enriched, having generated $\geq 10^9$ M_{sun} of dust in a period of only one to two billion years[17]. Very intense and continuous episodes of star formation ($\geq$1000 solar masses per year) are implied by the measured mm fluxes of thermal emission. Studies made with the present generation of sub-mm/mm telescopes have also established the presence of significant masses of dust in a few AGN[18] at $z \geq 6$, but the inability of these telescopes to go below a 10 mJy detection threshold in statistical samples has left many unanswered questions and significant inconsistencies between the results from different populations of radio galaxies and radio-quiet quasars[19]. Furthermore, given the small number of mm-wavelength detections of AGN, which are restricted to only the brightest examples, it has not been possible to constrain the evolving dust mass-function (or mm luminosity function) of optically and radio-selected quasars and radio-galaxies.

The low confusion-limits and high sensitivity of the LMT continuum instrumentation (AzTEC and SPEED) will allow the detection of dust masses more than 50 times less than the existing data, for large samples of AGN with different and well-controlled selection criteria. For example, the LMT will be able to compare the evolving dust masses in sub-samples of X-ray- and optically-selected quasars (e.g., from XMM, Chandra, SDSS, QUEST) with and without FIR detections from IRAS, ISO and Spitzer, against radio-selected radio-quiet quasars and steep-spectrum radio-loud sources. All these AGN samples will be compared against controls of inactive or passive elliptical and spiral galaxies in the local universe. Given the wide range of redshifts and AGN power (measured at X-ray, optical and radio-wavelengths), it will be possible to compare the evolution with redshift of the mm-wavelength properties of significant numbers of AGN with similar nuclear accretion-power, thereby minimizing the bias induced by the heating of dust grains by the direct radiation from the AGN. Conversely, it will also be possible, from the same parent sample, to consider the evolution of the dependence of the mm luminosity on non-thermal accretion power for subsamples of AGN selected in narrow redshift-slices in order to minimize the impact of evolution in any particular subsample (Figure 3.8).

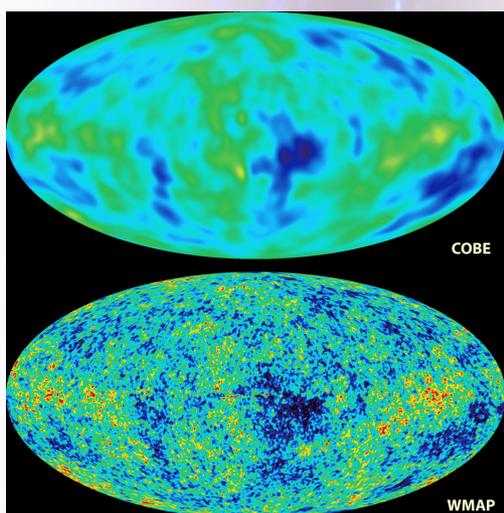*Figure 3.10 All-sky images of the infant universe, some 380,000 years after the Big Bang. In 1992 NASA's COBE mission first detected tiny temperature fluctuations (shown as color variations) in the young universe, a landmark discovery. The more recent WMAP image brings the COBE picture into sharper focus and has allowed the determination of basic cosmological parameters with unprecedented accuracy[23].*

Complementary studies of the molecular gas content will also be made for various molecular transitions with SEQUOIA, the Redshift Search Receiver, and the 1 mm and 2 mm SIS receivers (Chapter 8). These data will provide a measure of the physical properties (molecular gas-mass, gas temperature and density, dynamical mass, etc.) in the ISM of these AGN samples.
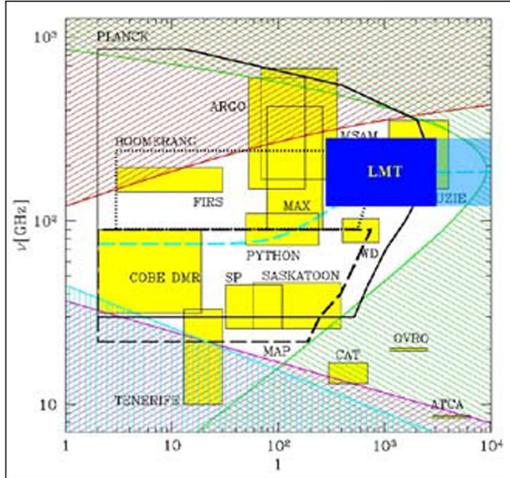

Figure 3.11 Telescope sensitivities as a function of angular scale (l ~ 120 /deg) and observing frequency. The opaque LMT region represents the practical limits with its initial instrumentation. The extended transparent blue region would be possible with future generations of 1000+ pixel bolometer arrays, given the spatial resolution afforded by the 50 m aperture[24].

All these future LMT observations will be placed in the context of the "unified scheme for AGN," which argues that there should be no difference between the properties of the AGN in radio-loud and radio-quiet samples (at a given extinction-corrected optical luminosity) except for those induced by an orientation-dependent effect (e.g., non spherically symmetric obscuration). The advantage of the LMT observations is that the mm-wavelength observations are insensitive to the obscuring effects of dust in the host galaxies of AGN. Hence LMT observations should not be adversely affected by source orientation, and mm-wavelength data for large, carefully constructed samples of AGN will provide important evidence to support or refute the "unified scheme" paradigm.

3.3.2 The Environment of AGN at Millimeter Wavelengths

The detection of the strong clustering of massive galaxies in the early universe provides a powerful test of the so-called "hierarchical scenario" for structure formation. A measure of the distribution of high-redshift massive (elliptical) galaxies, which are thought to trace the underlying dark matter distribution, offers one way to map out these over-densities. Hence the goal of many extragalactic mm surveys has been to search the high-redshift universe for clear signatures of the short, yet powerful bursts of obscured star formation (>> 100 solar masses per year) associated with the building of elliptical galaxies or their progenitors.

Instead of conducting blank-field mm surveys to find these random sites of massive-galaxy formation, however, the LMT can efficiently target fields in which we expect to sample high-density peaks in the underlying mass distribution. Observations towards high-redshift AGN are examples of these special environments, where, e.g., over-densities of Lyman-break galaxies

and mm sources have been found[20]. The most massive galaxies in the local universe are giant ellipticals which are also found in the centers of rich clusters. Since ellipticals host all known powerful radio-loud sources, then the study of high-redshift radio galaxies (HzRGs) provides the opportunity to study both the formation and evolution of massive elliptical galaxies and their proto-cluster environment. The most luminous radio-quiet quasars (RQQs) at high-redshift are also expected to be found inside massive ellipticals.

3.4 Detecting Cosmic Microwave Background Anisotropies with the LMT

The Cosmic Background Explorer (COBE) satellite demonstrated that the Cosmic Microwave Background (CMB) is both a perfect 2.73K blackbody (with fluctuations over the entire sky smaller than ~ 80 μK) and is isotropic[22]. This background is the primordial light from the surface of last scattering, the epoch at which the universe first cooled below the ionization temperature of hydrogen some 380,000 years after the Big Bang. As neutral atoms recombined from the hot plasma, radiation decoupled from matter, leaving the photons free to travel relatively unhindered until detected by CMB experiments some 13 billion years later.

Minute deviations from a perfectly smooth cosmic background are predicted, however, and have been observed at a level of one part in 100,000 ($dT/T \leq 10^{-5}$). Primary fluctuations, like the ripples seen on the surface of a pond, contain information about the conditions of the universe at the earliest moment that can be directly observed, the time of decoupling. Secondary fluctuations arise from the scattering of photons as they interact with gravitational potentials and sources of local ionization along the line of sight to the present-day observer. Previously, small single dish telescopes from satellite and balloon-borne platforms such as COBE, the Wilkinson Microwave Anisotropy Probe (WMAP), Maxima, and Boomerang, or ground-based interferometers such as the Cosmic Background Imager (CBI) or the Arcminute Cosmology Bolometer Array Receiver (ACBAR) have carried out measurements of the sky on large and small scales, respectively. The LMT, with its large primary aperture, will be able to bridge the gap between these previous experiments, due to the small beam (6-15 arcsec between 1.1 and 3 mm) and the excellent surface-brightness sensitivity (Figure 3.11). It is expected that in the future these LMT capabilities will be enhanced with a larger instantaneous field-of-view using filled-array focal-plane cameras.

3.4.1 Primary (Primordial) CMB Fluctuations

Inflation theory predicts that the primordial plasma had pressure and density inhomogeneities that grew according to the increasing scale-factor of the universe. These acoustic waves produce small temperature variations which are then observed as primary CMB fluctuations, "frozen" into the surface of last scattering at the epoch of decoupling. While the WMAP satellite has accurately measured these fluctuations over the entire sky down to an angular scale of $l \sim 600$ (about 0.2 degrees)[25], the LMT could measure the CMB fluctuations over a wide range of smaller angular scales, $300 < l < 3000$ (about 0.4 - 0.04 degrees), in reasonable amounts of integration time. These data would improve upon the accuracy of the high-l data from interferometers (e.g., ACBAR and CBI) as the LMT can image significantly larger areas. The overlapping angular scales with WMAP will provide important checks for the calibration and consistency of the LMT data. The higher-order acoustic features, and the steepness of the high-l cutoff, will be accurately measured in this regime, and will help to further constrain the fundamental cosmological parameters. Measurements of the CMB power-spectrum on the small angular scales probed by the LMT can be used to constrain the shape and Gaussian nature of the primordial spectrum of density fluctuations, which provide a test of the inflation theories, and also to provide an estimate of the epoch of hydrogen re-ionization in the early universe due to the formation of the first stars and powerful AGN.

3.4.2 Secondary CMB Fluctuations due to the Sunyaev-Zel'dovich Effect

A number of mechanisms can scatter the primordial CMB photons, some of which include plasma damping from the epoch of global re-ionization, scattering from moving gravitational potentials (i.e., large-scale flows), and gravitational lensing. The dominant source of secondary CMB fluctuations, caused by local ionization in clusters, will be detectable by the LMT.

Plasma in the inter-galactic medium within clusters interacts with CMB photons through inverse-Compton scattering, whereby hot electrons preferentially scatter lower-energy photons to higher energies. This *thermal* Sunyaev-Zel'dovich (S-Z) effect distorts the mm-wavelength spectrum of the CMB in the vicinity of clusters to produce a maximum decrement at 2.3 mm, a maximum increment at 0.85 mm, and a null at 1.4 mm. This distinctive spectral feature, combined with the sensitivity and resolution of the LMT, makes it possible to identify distant clusters (spectrally and spatially) from the confused foreground and background mm-wavelength radiation due to point-like galaxies and Galactic cirrus[26]. The amplitude of this effect is determined by the Compton-ionization y parameter, which

measures the scattering probability, and the density and temperature of the electrons. The combination of LMT observations of the S-Z effect at mm wavelengths with X-ray observations can constrain the mass of an individual cluster, a key physical parameter. Follow-up optical and IR imaging and spectroscopy of the galaxies associated with the identified clusters will provide measurements of their redshifts and velocity dispersions. This collective information will provide strong constraints on the growth of structure.

Furthermore, since the universe is transparent to mm-wavelength photons, and the strength of the S-Z effect is simply a distortion of the CMB and hence independent of redshift, then these LMT surveys for the S-Z signature will be unbiased with respect to distance, and they will therefore be an invaluable tool for studying the formation and evolution of large-scale structure at all epochs.

3.5 Gamma-ray Bursts (GRBs)

Gamma-ray bursts (GRBs) were discovered in the early 1970s by military satellites monitoring nuclear explosions in the Earth's atmosphere. Once the celestial origin of these events became established, their existence was

Figure 3.12 A gamma-ray burster: artist's conception of jets of high-energy particles emitted from a black hole at the center of a supernova shell[33].
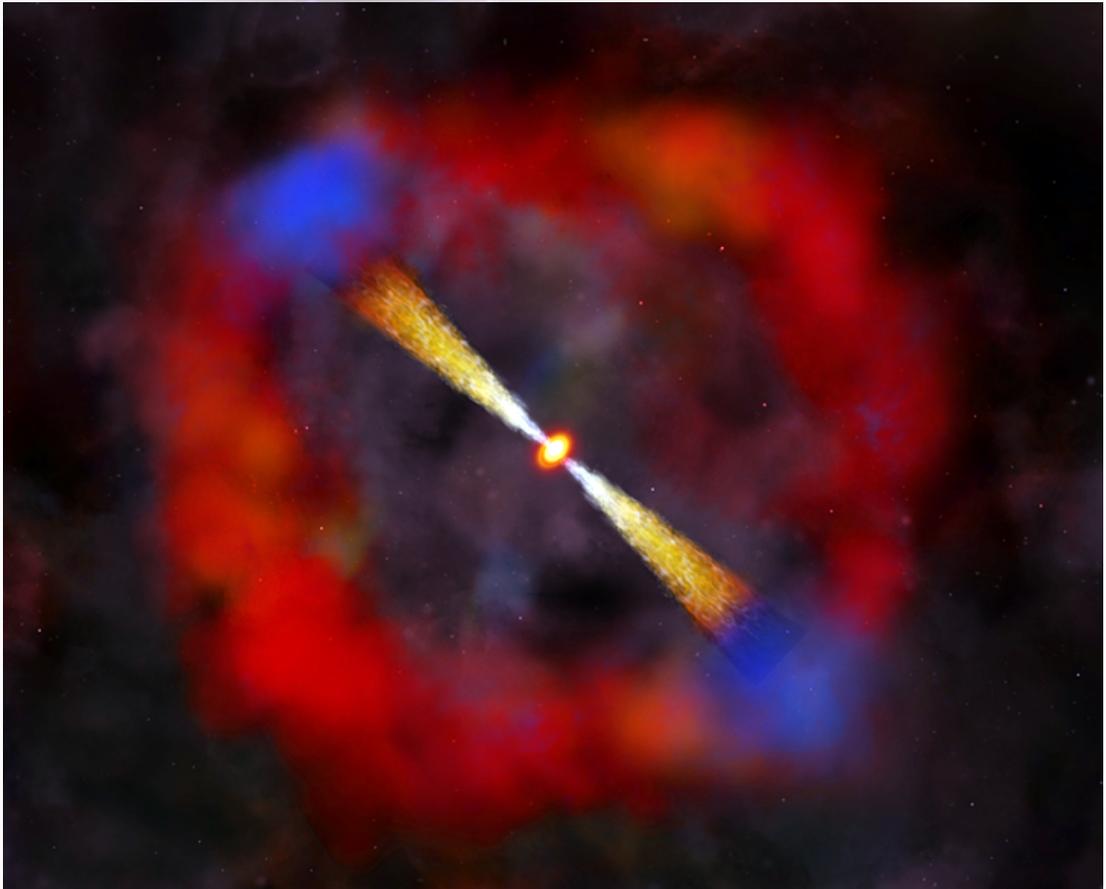
made public[27]. GRBs were for a long time among the most enigmatic phenomena in astrophysics. They are observed by instruments able to detect high-energy photons, namely X-rays and gamma-rays, which have to be satellite-borne to avoid absorption by the terrestrial atmosphere. GRBs originate from random positions in the sky, outshining any other celestial high-energy objects for short periods of time; their duration can be as short as a tenth of a second or as long as a few minutes. Except for a particular class of events called Soft Gamma-Ray Repeaters, GRBs do not happen twice in the same position on the sky. Since until very recently the telescopes able to detect them had a limited ability to locate sources in the sky, their origin remained a mystery for over two decades.

The Burst Alert and Transient Source Experiment (BATSE) on board the Compton Gamma-Ray Observatory (CGRO) was designed to detect a large number of GRBs, with the expectation of obtaining important clues about their origin. BATSE detected roughly one GRB per day, showing that they are evenly distributed across the sky, implying that they are a population of extragalactic objects[28]. The energy output originally inferred for these objects was 100 times higher than that of a supernova, the most violent event known in the universe at the time. However, more recent evidence indicates that GRBs are explosions where matter is ejected in very narrow jets and with incredible violence, at velocities very close to the speed of light[29]. But if matter is ejected only in narrow beams, the total energy output of the explosion is in fact much less than if matter were ejected in all directions.

In the late 1990s the Italian X-ray satellite Beppo-SAX showed that long-duration GRBs, those lasting more than two seconds, are often accompanied by a less intense, long-lasting X-ray emission[30]. These X-ray afterglows last for several hours, or even a few days, allowing a precise determination of the position of the GRB source in the sky, possible with low-energy imaging X-ray telescopes. The accurate positions permitted further follow-up observations with ground-based optical and radio telescopes, which have shown that GRBs occur in normal but distant galaxies, some of them at cosmological distances, as indicated by the large redshift of the host galaxy light[31]. A couple of GRB events have been observed to acquire the characteristics of a supernova, proving that GRBs are a particular type of supernova event[32]. At present it is believed that most supernovae explode isotropically, ejecting the matter of the progenitor star in all directions at speeds of about 10,000 km/s, while in GRBs matter is ejected practically 30 times faster in two very narrow beams. This is consistent with GRBs having been detected in very distant galaxies. In fact GRBs might become

an extremely powerful probe of the early universe, as they can be detected at distances larger than any other object by observers who happen to be aligned with either of the burst beams.

Even though supernovae and GRBs mark the death of a massive star, their positions indicate sites of star formation, as massive stars have a thousand times shorter lifetime than stars like the Sun. In this way the distant GRBs might be showing the first sites of star formation in the universe, with their high energy photons traveling for most of the universe's history before reaching our satellite X-ray and gamma-ray detectors. Once their location is unraveled, the most powerful telescopes on Earth can take up the challenge of observing and studying their host galaxy. In short, GRBs are believed to be associated with massive stars and therefore with star formation activity. On the other hand, most of the star formation at high redshifts seems to have occurred in deeply embedded dusty environments, prime targets for the LMT.

Present scientific issues concern the nature of GRB progenitors, the properties of their host galaxies, and their use as tracers of star formation at very high redshifts, as GRBs might point to galaxies at redshifts up to $z{\sim}15$. The LMT will operate in the same time frame as two important high-energy missions able to detect and properly locate gamma-ray bursts:

Figure 3.13 The first gamma ray burster X-ray afterglow discovered, GRB 970228, by the satellite observatory BeppoSAX[30].

Swift, launched in November 2004; and GLAST, to be launched in February 2007. The field of view of these high-energy space observatories covers 10% and 20% of the full sky, respectively, allowing the discovery of one GRB every two or three days on average. Swift and GLAST will provide initial locations of a few arcminutes, comparable to the field of view of the LMT. The few existing marginal detections of GRB host galaxies by mm and sub-mm telescopes show that the LMT will be able to detect tens of host galaxies per year, when guided by the accurate positions provided by Swift and GLAST. Afterglows have also been detected in the mm range, at the level of a few mJy at 0.85 mm and 1.2 mm. IRAM 30 m observations of GRB 991208 permitted it to locate where the ejecta became transparent to mm-photons and to follow its rapid evolution, providing powerful constraints on theoretical models[34]. The LMT will be able to perform deeper and longer observations of mm-afterglows of GRBs, allowing a clearer understanding of the interaction of the high-velocity ejecta with its near environment.
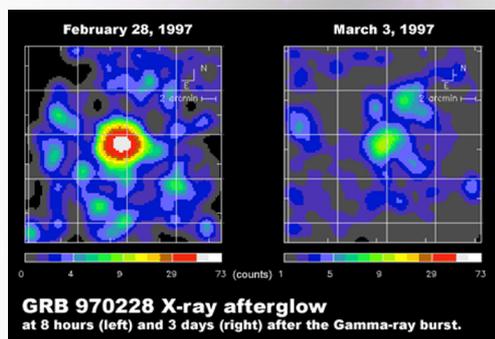
41

3.6 References

1. Chapin, E.L. (2004), "Constraining the History of High-Redshift Dust-Enshrouded Star-Formation with Baloon-Borne and Ground-Based Sub-Millimetre Surveys," Doctoral Dissertation, INAOE.

2. Credit: D.H. Hughes, INAOE.

3. Smail, I. et al. (1997), "A Deep Sub-millimeter Survey of Lensing Clusters: A New Window on Galaxy Formation and Evolution," *Astrophys. J., 490*, L5.

4. Hughes, D.H. et al. (1998), "High-redshift star formation in the Hubble Deep Field revealed by a submillimetre-wavelength survey," *Nature, 394*, 241.

5. Hughes, D.H. & Aretxaga, I., (2005), "Understanding the History of Obscured Star Formation in the High-redshift Universe with Coordinated GTC and LMT Surveys," in "II International Workshop on Science with the GTC: Science with GTC 1st-light Instruments and the LMT," eds. J.J. Gonzalez and J.M. Rodriguez-Espinosa, *Rev. Mex. Astron. Astrophys. (Ser. Conf.)*, in press.

6. Adapted from Hughes, D.H. et al. (2005), "Resolving the FIR-Submillimetre Extragalactic Background from Dome C, Anctartica," in "Dome C Astronomy/Astrophysics Meeting," *EAS Publ. Ser.*, in press.

7. E.g., Yun, M.S. & Carilli, C.L. (2002), "Radio-to-Far-Infrared Spectral Energy Distribution and Photometric Redshifts for Dusty Starburst Galaxies," *Astrophys. J., 568*, 88.

8. Chapman, S.C. et al. (2003), "A median redshift of 2.4 for galaxies bright at submillimetre wavelengths," *Nature, 422*, 695.

9. Aretxaga, I. et al. (2003), "Breaking the 'redshift deadlock'-II. The redshift distribution for the submillimetre population of galaxies," *MNRAS, 342*, 759.

10. Greve, T.R. et al. (2005), "An interferometric CO survey of luminous submillimetre galaxies," *MNRAS, 359*, 1165.

11. Credit: M. Yun, UMass Amherst/FCRAO.

12. Hughes, D.H. et al. (1993), "Thermal Dust Emission from Quasars - Part One - Submillimetre Spectral Indices of Radio Quiet Quasars," *MNRAS, 263*, 607.

13. Dunlop, J.S. et al. (1993), "Infrared Imaging of the Host Galaxies of Radio-Loud and Radio-Quiet Quasars," *MNRAS, 264*, 455.

14. E.g., Aretxaga, I. et al. (1998), "Multicolour imaging of z=2 QSO hosts," *MNRAS, 296*, 643.

15. Credit: J. Bahcall (IAS), M. Disney (University of Wales) and NASA.

16. Gebhardt, K, et al. (2000), "Black Hole Mass Estimates from Reverberation Mapping and from Spatially Resolved Kinematics," *Astrophys. J. Lett.*, 543, L5.

17. Archibald, E.N. et al. (2002), "Coupled spheroid and black hole formation, and the multifrequency detectability of active galactic nuclei and submillimeter sources," *MNRAS, 336*, 353.

18. Robson, I. et al. (2004), "Submillimetre observations of z > 6 quasars," *MNRAS, 351*, L29.

19. Priddey, R.S. et al. (2003), "The SCUBA Bright Quasar Survey (SBQS) - II. Unravelling the quasar epoch at submillimetre wavelengths," *MNRAS, 339*, 1183.

20. Stevens, J.A. et al. (2003), "Sub-mm imaging of Distant Radio Galaxies: Witnessing the Formation of Massive Cluster Ellipticals," *Nature, 425*, 264.

21. Governato, F. et al., (1998), "The seeds of rich galaxy clusters in the Universe," *Nature, 392*, 359.

22. Smooth, G.F. et al. (1992), "Structure in the COBE differential microwave radiometer first-year maps," *Astrophys. J., 396*, L1.

23. Credit: Scientific Group, NASA/WMAP (http://map.gsfc.nasa.gov/)

24. Montana, A. (2002), "Fluctuations and Anisotropies in the Cosmic Microwave Background," Master's Thesis, INAOE.

25. Bennett, C.L. et al. (2003), "First Year Wilkinson Microwave Anisotropy Probe (WMAP) Observations: Preliminary Maps and Basic Results," *Astrophys. J. Suppl.*, *148*, 1.

26. Aragón Calvo, M. A. (2002), "Simulations of the Sunyaev-Zel'dovich Effect, and their Application to Future Millimetre-Wavelength Experiments," Master's Thesis, INAOE.

27. Klebesadel, R.W. et al. (1973), "Observations of Gamma-Ray Bursts of Cosmic Origin," *Astrophys. J., 182*, L85.

28. Briggs, M.S. et al. (1996), "BATSE Observations of the Large-Scale Isotropy of Gamma-Ray Bursts," *Astrophys. J., 495*, 40.

29. Rees, M.J. & Mészáros, P. (1992), "Relativistic fireballs — Energy conversion and time-scales," *MNRAS, 258*, 41.

30. Costa, E. et al. (1997), "Discovery of an X-ray afterglow associated with the gamma-ray burst of 28 February 1997," *Nature, 387*, 783.

31. Kulkarni, S.R. et al. (1998), "Identification of a host galaxy at redshift z = 3.42 for the gamma-ray burst of 14 December 1997," *Nature, 393*, 55.

32. Mészáros, P. (2003), "Gamma-ray bursts: The supernova connection," *Nature, 423*, 809.

33. Credit: CXC/M. Weiss.

34. Galama, T.J. et al. (2000), "The Bright Gamma-Ray Burst 991208: Tight Constraints on Afterglow Models from Observations of the Early-Time Radio Evolution," *Astrophys. J., 541*, L45.

35. Rawlings, S. et al. (2004), "Submillimetre photometry of typical high-redshift radio quasars," *MNRAS, 351*, 696.